FREQUENCY DEPENDENCY OF MULTIPATH FADING OVER THE SEA UNDER DUCTING

Part I: SIMULATION RESULTS FOR REFRACTIVITY PROFILES' PARAMETERS INFLUENCE

Irina SIRKOVA

Laser Radars Lab, Institute of electronics
Bulgarian Academy of Sciences, Tzarigradsko chaussee 72, 1784 Sofia, Bulgaria

irina@ie.bas.bg

Abstract

Over water microwave propagation is often affected by the presence of evaporation duct. The tropospheric ducting is one of the major causes for multipath propagation. The ducting propagation mechanism is known to be highly frequency dependent whereas the prediction methods for multipath fading distribution suggest a rather slight dependence on frequency. In order to check this discrepancy, Part I of this work deals with the influence of the variations of important parameters of the evaporation duct log-linear refractivity profile on the frequency dependency of multipath fading. The refractivity profiles serve as input to the parabolic equation method which provides a full-wave solution to the path loss problem. Ten frequencies of microwave range are used in four hypothetical over the sea links. The results are presented in form of path loss standard deviation versus frequencies for fixed ranges.

1. INTRODUCTION

The propagation conditions in coastal and maritime regions are often complicated by changes in the tropospheric refractive index leading to formation of tropospheric ducts [1]. This peculiarity makes the preliminary assessment of microwave propagation in those regions difficult and subject to significant errors [2]. One of the consequences of the ducts' formation is the multipath propagation and, accordingly, the multipath fading [3]. The assessment of fading is an important part of performance predicting of radio communication links. To achieve the necessary accuracy in performance predicting, sophisticated propagation channel modelling methods are applied which account simultaneously for terrain irregularities, clear air propagation mechanisms, and antenna patterns. Among them the Parabolic Equation (PE) method [4] has become one of the most widely used to solve microwave propagation problems especially in complicated environments such as tropospheric ducting [4, 5]. Despite the variability of the marine boundary layer [6], for practical purposes one usually assumes lateral homogeneity for the refractivity and applies a single profile, approximated to account for the average behaviour of the modified refractivity $M(z)$ with height z, as environmental input to the PE. Special attention is paid to the modelling of $M(z)$ for evaporation duct due to its frequent occurrence and particular importance in coastal and maritime regions. Most often the evaporation duct is modelled by log-linear height profile of the modified refractivity M [7]:

$$M(z) = M_0 + c_0\left[z - z_d \ln\left(\frac{z + z_0}{z_0}\right)\right] \quad , \qquad (1)$$

where $M_0 = M(z = 0)$, z_0 is the aerodynamic roughness parameter usually taken to be 1.5×10^{-4} m [4], z_d is the duct height corresponding to the height at which $dM/dz = 0$, c_0 is the critical potential refractivity gradient [8] usually taken to be 0.13. The physics behind this profile, based on the Monin–Obukhov similarity theory, is explained in [4, 7]. With above values of parameters c_0 and z_0, (1) has been obtained assuming thermally neutral troposphere stratification and does not account for the stability effects on the M profile. This most usual form of evaporation duct log-linear M profile is governed by one parameter - the duct height, z_d, which determines the other important duct parameter, the M-deficit, $\Delta M = M(z_d) - M_0$. Recently attempts at improving (1) have been made by changing the slope in different parts of the log-linear curve [8, 9], thus making it to better fit the experimental profiles and, hence, include the influence of tropospheric stability. In [8] the parameters of evaporation duct refractivity model (1) have been optimized using radiosonde data. This study has shown that the best log-linear model formulation would include, except for the most important duct parameter z_d, also duct curvature and mixed layer slope (mixed layer is the well-mixed by turbulent mixing layer above the duct). In (1) c_0 and z_0 are parameters responsible for the profile curvature (c_0 changes the radius of curvature surrounding the duct whereas z_0 changes the curvature below the duct only [8]). Those parameters influence also the *M*-deficit under the same z_d.

The ducting propagation mechanism is highly frequency dependent whereas the prediction methods for multipath fading distribution on line-of-sight links suggest a rather slight dependence on frequency [10, 11]. In order to check this discrepancy, this work studies how the parameters of profile (1) reflect on the frequency dependency of (large-scale) multipath fading in the case of microwave propagation over the sea under evaporation duct conditions. The evaporation duct model (1), with varying parameters z_d and c_0, serves as input to the PE method [4] to compute the path loss' standard deviation in the areas of interests. Ten frequencies of microwave range are used in four hypothetical over the sea line-of-site links.

2. DESCRIPTION OF THE METHOD

The PE method is applied as implemented in "Advanced propagation model (APM) Computer software configuration item (CSCI) documents", Space and Naval Warfare Systems Center Tech. Doc. 3145, San Diego, CA, 2002. Those routines make use essentially of the 2D narrow-angle forward-scatter scalar PE, (2), which provides a full-wave solution to the path loss problem:

$$\frac{\partial u(x,z)}{\partial x} = \frac{i}{2k}\frac{\partial^2 u(x,z)}{\partial z^2} + \frac{ik}{2}\left(m^2(x,z)-1\right)u(x,z). \quad (2)$$

Details on the derivation of (2), its validation and use for electromagnetic (EM) field calculations under tropospheric ducting conditions are largely reported in the literature [4, 5] and will not be repeated here. In (2) k is the free-space wave number, $m = M \times 10^{-6}+1$ is the modified refractive index, $u(x,z)$ is a slow-varying along the preferred propagation direction, x, function related to the corresponding to the polarization transverse EM field component, x and z stay for range and altitude. The popularity of (2) is related to its easy numerical solution through marching algorithms. In addition to boundary conditions, (2) requires knowledge of initial field [4]. The drawback of (2) is the neglect of backscattering. The studied microwave propagation problem is characterized by EM field variations over scales much larger than the wavelength, grazing incident angles, and smooth variation of the tropospheric refractive index with x; under these conditions the forward-propagated field plays dominant role and this assures the applicability of (2).

The initial field required to start the calculations is provided by horizontally polarized Gaussian beam source with pattern factor given by (3) where θ_0 and θ_s are the half power beamwidth and the antenna elevation angle. Smooth perfect conducting underlying surface (sea) is assumed. The results are presented in the form of standard deviation of the path loss (*PL* in dB, see (4)) in the area of interest versus frequency for fixed range.

$$F(\theta) = \exp\left[\frac{\ln(0.707)(\theta-\theta_s)^2}{\left(\theta_0/2\right)^2}\right] , \quad (3)$$

$$PL = 20\log\left(\frac{4\pi r}{\lambda}\right) - PF . \quad (4)$$

In (4) λ is the free-space wavelength, r is the distance between the corresponding points and *PF* is the pattern propagation factor defined as the square of the ratio of the electric field amplitude E received at a given point under specific conditions to the amplitude of the electric field E_0 received under free-space conditions with the beam of the transmit antenna directed toward this given point [4].

3. RESULTS AND DISCUSSION

For every frequency the *PL* is calculated versus height for fixed ranges R = 20 km, R = 40 km for four hypothetical links: A) z_t = 40 m, $\theta_0 = 5^0$; B) z_t = 15 m, $\theta_0 = 5^0$; C) z_t = 40 m, $\theta_0 = 1^0$; D) z_t = 15 m, $\theta_0 = 1^0$, where z_t stays for the transmitter height. Three different values for c_0 are used: $c_0 = 0.13$, $c_0 = 0.11$ and $c_0 = 0.19$, the last two accounting for the deviation from the thermally neutral troposphere stratification. For all cases $\theta_s = 0^0$ in (3). The parameter z_0 is kept equal to 1.5×10^{-4} m in all reported examples. The receiver height is supposed to start from z_r = 5 m and go up to 150 m. This area of interest is divided in two parts: z_1 from 5 m to the top of evaporation layer, defined here as $z_L = 2z_d$, see [8], and z_2 which ranges from the evaporation layer height z_L up to 150 m. The frequencies are shown in Table 1. Those frequencies belong to the ranges used for coastal and maritime radars (lower ranges) and fixed and mobile links (upper ranges). The results are presented in form of *PL* standard deviation versus frequencies.

Table 1. Frequencies used, GHz

2.4	3.1	4.5	5.6	7.1	8.4	9.3	13.4	15.4	19.7

Figure 1 shows range-independent duct with z_d = 35 m = ct over the entire distance of *R* = 20 km for link A and the two areas of interest, z_1 and z_2.

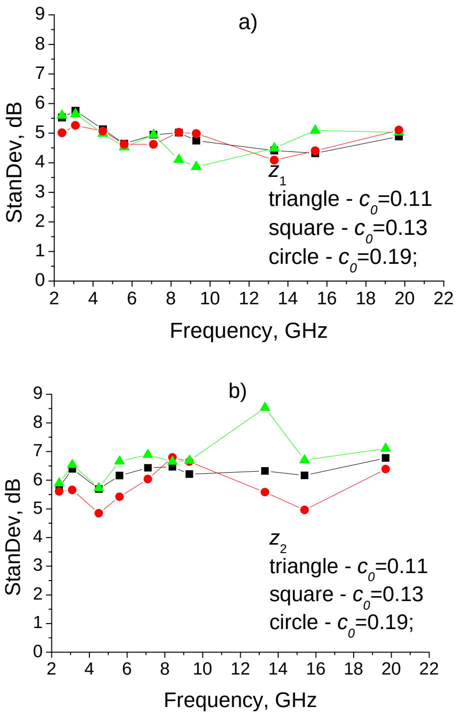

Figure 1. Range-independent duct: z_d = 35 m, *R* = 20 km, link A

Figure 2 reports similar results but for z_d = 10 m = ct and link B. On both figures one can see comparison for three different values of c_0. On Fig. 3, which refers to link C, the *PL* standard deviation for z_d = 35 m duct is compared to standard troposphere conditions at distance *R* = 40 km. As it is seen from Figs. 1-3, the frequency dependency of PL standard deviation is rather slight and has similar character for the three values of c0; it is higher in area z_1, especially for the lower frequencies, see Fig. 2a). This may be due to the fact that the lower frequencies are not well trapped in the thinner duct from Fig. 2. For the three Figs., both z_t and z_r are submerged in the evaporation layer (z_t, $z_r < z_L$) which determines the more pronounced influence of the duct for area z_1 than for z_2.

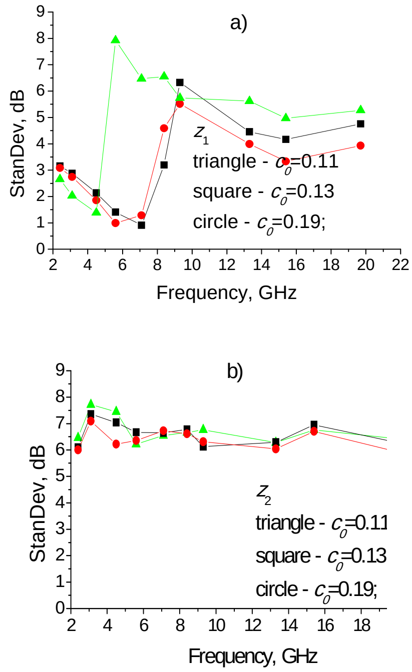

Figure 2. Range-independent duct: z_d = 10 m, *R* = 20 km, link B

Figure 3 differs from Fig. 1 through the greater distance (*R* = 40 km) at which the *PL* is computed and the narrower antenna beam ($\theta_0 = 1^0$). The longer the distance, the higher the duct influence; on the other hand the larger antenna beam and shorter distance determine the predominant role of the reflections from the underlying surface - this could explain the "smoothed" frequency dependence on Fig. 3 compared to Fig. 1. All studied frequencies are well trapped and strongly guided in the "thick" duct on Fig. 3 which determines the lower scattering and, hence, the lower values of standard deviation for the ducting in area z_1 in comparison to standard troposphere case. As for z_2 on Fig. 3, in this area the slope of the *M* profile above z_L is (almost) the same for the duct and standard troposphere which determines closer values for standard deviation in both cases in z_2.

The frequency dependency of standard deviation for range-dependent duct in sense that the start refractivity profile has c_0 = 0.13 which changes to c_0 = 0.19 at the mid path has also been studied; the results (not reported here) indicated (once again) the rather week influence of the variation of c_0 (except for the lowest frequencies), especially in area z_2.

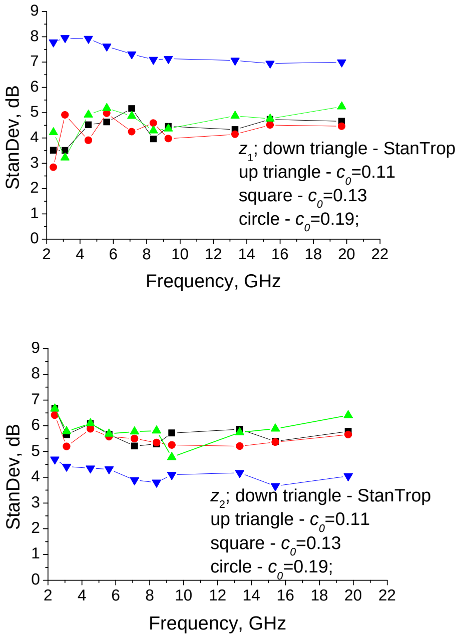

Figure 3. Range-independent duct: z_d = 35 m, *R*=40 km, link C

Further, on Fig. 4, another range-dependent case is demonstrated by changing the z_d parameter in the middle of the path from initial z_d = 10 m to z_d = 15 m, c_0 = 0.19 = ct, R = 20 km, link C. As expected, on Fig. 4 for the area z_1 the change in z_d almost does not reflect on the frequency dependency because z_t for link C is above evaporation layer z_L for both z_d values. The influence of increased z_d is higher in the area z_2.

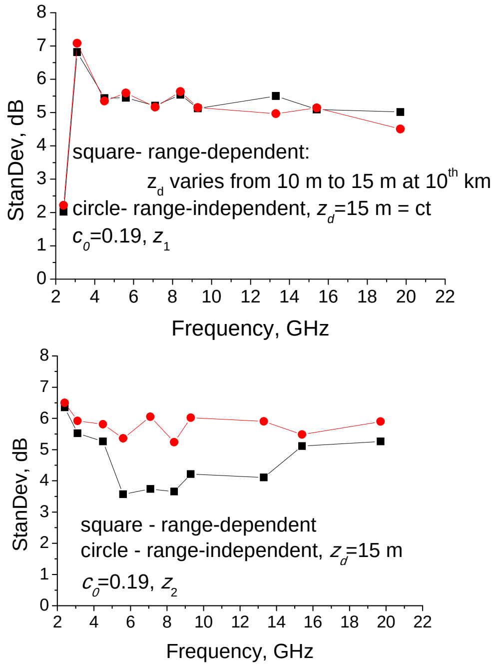

Figure 4. Comparison between range-dependent and range independent duct, R = 20 km, link C

4. CONCLUSION

On the basis of Figs. 1-4 the following concluding remarks may be drawn:

- in the studied limits, the results support the applicability of profile (1) with c_0 = 0.13;
- in general, the frequency dependency of multipath fading under ducting conditions modelled by (1) for smooth sea surface is rather slight and appears to be in accordance with the slight influence of the frequency dependent factor in widely applied prediction methods [2, 10, 11]. More attention is to be paid to lower frequencies when ducts with low z_d are present. The particular case when z_t is between z_d and evaporation layer z_L needs additional studies.

5. ACKNOWLEDGMENTS

This work was supported in part by the Ministry of Education and Science of Bulgaria under grant agreement № D01-151/2018.

REFERENCES

[1] *ITU-R P.453-9, "The Radio Refractive Index: its Formula & Refractivity Data", 2003.*

[2] *R. L. Olsen and T. Tjelta, "Worldwide Techniques for Predicting the Multipath Fading Distribution on Terrestrial LOS Links: Background and Results of Tests",* IEEE Trans*, Vol. AP-47, No. 1, 1999, 157-170.*

[3] *S. R. Saunders and A. Aragon-Zavala,* Antennas and Propagation for Wireless Communication Systems*, John Wiley & Sons, 2nd edition, 2007.*

[4] *M. Levy,* Parabolic Equation Methods for Electromagnetic Wave Propagation*, IEE electromagnetic waves series 45, UK, 2000.*

[5] *I. Sirkova, "Brief Review on PE Method Application to Propagation Channel Modeling in Sea Environment",* CEJE*, Vol. 2, No. 1, 2012, 19-38.*

[6] *B. W. Atkinson and M. Zhu, "Coastal Effects on Radar Propagation in Atmospheric Ducting Conditions",* Meteorological Applications*, Vol. 13, 2006, 53–62.*

[7] *R. A. Paulus, "Practical application of an evaporation duct model",* Radio Sci.*, Vol. 20, 1985, 887–896.*

[8] *J. T. Saeger, N. G. Grimes, H. E. Rickard, and E. E. Hackett, "Evaluation of Simplified Evaporation Duct Refractivity Models for Inversion Problems",* Radio Sci.*, Vol. 50, No. 10, 2015, 1110–1130.*

[9] *J.-P. Zhang, Z.-S. Wu, Q.-L. Zhu, and B. Wang, "A Four-Parameter M-profile Model for the Evaporation Duct Es-*

timation from Radar Clutter", PIER*, Vol. 114, 2011, 353-368.*

[10] *R.L. Olsen, T. Tjelta, L. Martin, and B. Segal, "World-wide Techniques for Predicting the Multipath Fading Distribution on Terrestrial LOS Links: Comparison with Regional Techniques",* IEEE Trans*, Vol. AP-51, No. 1, 2003, 23-30.*

[11] *ITU-R P.530-9, "Propagation Data and Prediction Methods Required for the Design of Terrestrial Line-of-Sight Systems", 2001.*